

# New Approach for Designing Single-Chain Magnets: Organization of Chains via Hydrogen Bonding between Nucleobases

Wei-Xiong Zhang,<sup>\*,§</sup> Takuya Shiga,<sup>†</sup> Hitoshi Miyasaka,<sup>‡</sup> and Masahiro Yamashita<sup>\*,§</sup>

<sup>§</sup>Department of Chemistry, Graduate School of Science, Tohoku University, 6-3 Aramaki-Aza-Aoba, Aobaku, Sendai 980-8578, Japan

<sup>†</sup>Graduate School of Pure and Applied Sciences, University of Tsukuba, 1-1-1 Tennodai, Tsukuba 305-8571, Japan

<sup>‡</sup>Department of Chemistry, Division of Material Sciences, Graduate School of Natural Science and Technology, Kanazawa University, Kakuma, Kanazawa 920-1192, Japan

## S Supporting Information

**ABSTRACT:** Two one-dimensional (1D) manganese complexes,  $[\text{Mn}_2(\text{naphmen})_2(\text{L})](\text{ClO}_4)_2 \cdot 2\text{Et}_2\text{O} \cdot 2\text{MeOH} \cdot \text{H}_2\text{O}$  (**1**) and  $[\text{Mn}_2(\text{naphmen})_2(\text{HL})](\text{ClO}_4)_2 \cdot \text{MeOH}$  (**2**), were synthesized by using a bridging ligand with a nucleobase moiety, 6-amino-9- $\beta$ -carboxyethylpurine, and a salen-type manganese(III) dinuclear complex,  $[\text{Mn}_2(\text{naphmen})_2(\text{H}_2\text{O})_2](\text{ClO}_4)_2$  (naphmen<sup>2-</sup> = *N,N'*-(1,1,2,2-tetramethylethylene)bis(naphthylideneiminato) dianion). In **1** and **2**, the carboxylate-bridged Mn<sup>III</sup> dinuclear units are alternately linked by two kinds of weak Mn $\cdots$ O interactions into 1D chains. As a result, canted antiferromagnetic and ferromagnetic interactions are alternately present along the chains, leading to a 1D chain with non-cancellation of anisotropic spins. Since the chains connected via H-bonds between nucleobase moieties are magnetically isolated, both **1** and **2** act as single-chain magnets (SCMs). More importantly, this result shows the smaller canting angles hinder long-range ordering in favor of SCM dynamics.

Single-molecule magnets (SMMs) and single-chain magnets (SCMs) exhibit quantum magnetism and magnetic relaxation phenomena in contrast to bulk magnets.<sup>1</sup> To construct SMMs, magnetically isolated molecules must have large spin ground states and uniaxial magnetic anisotropy.<sup>2</sup> In general, SMMs are prepared by forming discrete clusters of paramagnetic centers with high magnetic anisotropy via ligands that can mediate the magnetism, causing a higher spin ground state. On the other hand, SCMs are composed of one-dimensional (1D) chain complexes with magnetic coupling along the chain and non-cancellation of the uniaxial anisotropic spins. The chains should be as magnetically isolated as possible, meaning that the magnetic interchain interactions must be very weak compared to intrachain coupling in order to avoid the stabilization of 3D magnetic ordering.<sup>3</sup> Thus, large counterions and bulky molecules have been used to prepare SCMs.<sup>4</sup> In this paper, we propose a new synthetic approach for preparing SCMs, in which H-bonded nucleobase groups are used to isolate/arrange 1D SCMs in a crystal. In this study, we used 6-amino-9- $\beta$ -carboxyethylpurine (HL) as a bridging ligand and exploited the H-bonding ability of adenine group as the nucleobase moiety to link the chains.<sup>5</sup> The salen-type Mn<sup>III</sup>

complex  $[\text{Mn}_2(\text{naphmen})_2(\text{H}_2\text{O})_2](\text{ClO}_4)_2$  (naphmen<sup>2-</sup> = *N,N'*-(1,1,2,2-tetramethylethylene)bis(naphthylideneiminato) dianion), which has a large magnetic anisotropy, was used as a building block.<sup>6</sup>

The 1D Mn complex  $[\text{Mn}_2(\text{naphmen})_2(\text{L})](\text{ClO}_4)_2 \cdot 2\text{Et}_2\text{O} \cdot 2\text{MeOH} \cdot \text{H}_2\text{O}$  (**1**) was synthesized by reacting HL and triethylamine with the Mn<sup>III</sup> complex  $[\text{Mn}_2(\text{naphmen})_2(\text{H}_2\text{O})_2](\text{ClO}_4)_2$  (see SI).  $[\text{Mn}_2(\text{naphmen})_2(\text{HL})](\text{ClO}_4)_2 \cdot \text{MeOH}$  (**2**) was obtained by a similar reaction without triethylamine; namely, the adenine group of **2** was protonated. From single-crystal X-ray crystallography, both complexes crystallized in the triclinic space group *P* $\bar{1}$  (see SI). In their asymmetric units, two crystallographically independent Mn(naphmen) units, with the naphmen ligands in a quasi-plane chelate mode, are bridged by a carboxylate group in a *syn-anti* mode (Figures S1, S2). As shown in Figure 1, the resulting carboxylate-bridged Mn<sup>III</sup> dinuclear units are alternately linked by two types of weak Mn $\cdots$ O<sub>Ph</sub> coordination interactions, which form out-of-plane dimers often observed in salen-type Mn<sup>III</sup> SMMs.<sup>7</sup> As a result, a 1D chain structure with a  $[\cdots\text{Mn}-(\text{CO}_2)-\text{Mn}\cdots(\text{O}_{\text{Ph}})_2\cdots]$  repeat was formed along the (011) crystallographic axis in **1** and the *c* axis in **2**. Both compounds have H-bonds between adenine moieties of adjacent chains (Figure 1, right). In **1**, the adenine groups interact with the adenine groups of neighboring chain through the proton of the amine group (N9) and the 1-position nitrogen atom (N5\*). In **2**, however, adenine groups are protonated at the 1-position nitrogen atom (N5). Therefore, H-bonds form between a proton of amine group (N9) and the 7-position nitrogen atom (N8\*). These H-bonds differ from those of the complementary base pair in DNA and link the chains to form 2D layers in the *bc* plane for **1** and the (220) crystallographic plane for **2** (Figure S3). The counterions and/or the disordered solvent molecules fill the space between the 2D layers. The closest atomic distance between the paramagnetic metal ions of adjacent chains is 12.642(3) Å for **1** and 10.905(1) Å for **2**. As a result, the H-bonds and solvent molecules effectively separate the chains, in contrast to reported analogues with no H-bonds and solvent molecules between magnetic chains.<sup>8</sup> H-bonding between the chains causes a

Received: January 6, 2012

Published: April 9, 2012



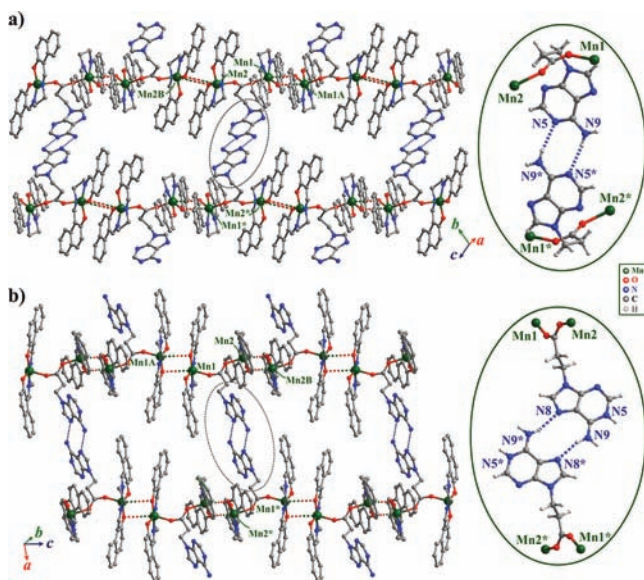


**Figure 1.** 1D chains of (a) **1** and (b) **2**. H atoms, solvent molecules,  $\text{ClO}_4^-$  anions, and the methyl groups of the naphtmen units have been omitted for clarity. Details of H-bonding between the adenine moieties are shown on the right. Symmetry operations: for **1**, (A)  $-x+2, -y, -z$ ; (B)  $-x+2, -y+1, -z+1$ ; (\*)  $-x+2, -y, -z+1$ ; for **2**, (A)  $-x, -y+1, -z$ ; (B)  $-x, -y+1, -z+1$ ; (\*)  $-x+2, -y, -z+1$ .

dramatic difference in the magnetic properties of the analogues and **1** and **2**.

Magnetic measurements were performed on ground polycrystalline samples of **1** and **2** in a dc field of 1 kOe. As shown in Figure 2a, the  $\chi T$  values at 300 K were 5.96

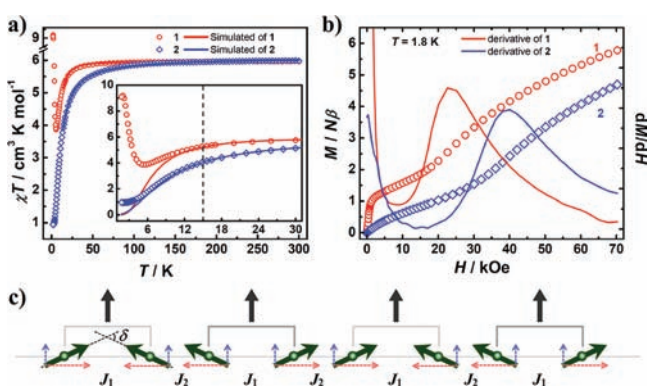


**Figure 2.** (a) Variable-temperature dc magnetic susceptibility data for **1** (red) and **2** (blue) collected in an applied field of 1 kOe. The solid line is a fit of the data, as described in the text. (b) Field-dependent magnetizations and its derivative of **1** (red) and **2** (blue) at 1.8 K. (c) Diagram of the spin canting in **1** and **2**. The green arrows represent the spins of the  $\text{Mn}^{\text{III}}$  ions, which could be divided into uncompensated and compensated components shown as blue and red dashed arrows, respectively. The resulting net magnetic moments (black arrows) in the AF dimers are parallel to each other in a 1D arrangement.

$\text{cm}^3 \cdot \text{mol}^{-1} \cdot \text{K}$  for **1** and  $5.98 \text{ cm}^3 \cdot \text{mol}^{-1} \cdot \text{K}$  for **2**, close to the value expected for two uncorrelated  $\text{Mn}^{\text{III}}$  ions ( $6.00 \text{ cm}^3 \cdot \text{mol}^{-1} \cdot \text{K}$ ). The  $\chi T$  values gradually decreased with decreasing temperature, reaching  $3.87 \text{ cm}^3 \cdot \text{mol}^{-1} \cdot \text{K}$  at 5.4 K for **1** and  $0.98 \text{ cm}^3 \cdot \text{mol}^{-1} \cdot \text{K}$  at 3.0 K for **2**. When the temperature was lowered further, the  $\chi T$  value for **1** gradually

increased, whereas that for **2** scarcely changed. As shown in Figure 1, two different intrachain magnetic bridges are alternately present along the chain:<sup>9</sup> *syn-anti* carboxylate bridges (labeled as  $J_1$ ), which usually pass antiferromagnetic (AF) interactions, and phenolate bridges (labeled as  $J_2$ ), which usually pass ferromagnetic (F) interactions due to accidental orthogonality of magnetic orbitals.<sup>7</sup> The magnetic susceptibility data in the higher temperature region suggest that  $J_1$  is dominant in both **1** and **2**.

To clarify the magnetic interactions, the data above 14 K were analyzed by using a Heisenberg dimer model with  $S = 2$  and the zero-field splitting term ( $D$ ) for each  $\text{Mn}^{\text{III}}$  ion (spin Hamiltonian  $\mathbf{H} = -2J_1 S_1 S_2 + 2D[S_z^2 - S(S+1)/3]$ ,  $S_1 = S_2 = 2$ ). The analysis afforded  $g = 1.99$ ,  $J_1 = -0.97 \text{ K}$ ,  $D = -3.21 \text{ K}$ , and the residual factor  $R = \sum(\chi_{\text{obs}} T - \chi_{\text{cal}} T)^2 / \sum(\chi_{\text{obs}} T)^2 = 2.4 \times 10^{-5}$  for **1** and  $g = 2.01$ ,  $J_1 = -1.48 \text{ K}$ ,  $D = -1.46 \text{ K}$ , and  $R = 3.2 \times 10^{-6}$  for **2**. The  $D$  values are consistent with the typical value for  $\text{Mn}^{\text{III}}$  salen analogues and the presence of Jahn–Teller distortion in these compounds.<sup>6,10</sup> The negative  $J_1$  values further confirm that AF interactions through the single *syn-anti* carboxylate bridges are dominant and are consistent with the distinct inflection points, at which the fields ( $H_{\text{ex}} = 23 \text{ kOe}$  for **1** and  $40 \text{ kOe}$  for **2**, Figure 2b) overwhelm the AF interactions. The inflection points make it possible to roughly estimate the AF interactions using  $2zJ_1 S^2 = gS\mu_B H_{\text{ex}}$  with  $z = 1$  and  $g = 2.0$ :  $|J_1| = 0.77 \text{ K}$  for **1** and  $1.32 \text{ K}$  for **2**, similar to the values estimated from simulations of  $\chi T$ .

No inversion center exists between Mn1 and Mn2 ions linked by the *syn-anti* carboxylate bridges. In addition, their Jahn–Teller axes are not parallel to each other but form an angle  $\theta$  of  $46.1(1)^\circ$  in **1** and  $23.6(1)^\circ$  in **2**, estimated from the structure in Figure S4. Thus, a canted arrangement of spins is formed due to the antisymmetric magnetic exchange interactions in the carboxylate-bridged dinuclear units, leading to small net magnetic moments.<sup>11</sup> It should be pointed out that the canting angle  $\delta$  in Figure 2c is smaller than  $\theta$  because the AF interactions cause the spin vectors to align antiparallel; it was estimated from  $J_1$ ,  $D$ , and  $\theta$  to be  $29^\circ$  for **1** and  $7.7^\circ$  for **2**.<sup>12</sup> As shown in Figure 2c, the resulting small net magnetic moments are correlated ferromagnetically with  $J_2 > 0$  along the chain. Thus, the values of  $\chi T$  for **1** increased at lower temperatures, although they remained constant for **2** due to a very small net magnetic moment compared to that for **1** (vide infra). These observations satisfy one of the requirements for SCMs: 1D chains with magnetic coupling along the chain and non-cancellation of the anisotropic spins.

Ac magnetic susceptibility measurements on powder samples of **1** and **2** were performed in the temperature range of 1.8–4.0 K (Figure 3). Both in-phase ( $\chi'$ ) and out-of-phase ( $\chi''$ ) components were dependent on the frequency, and their peak maxima shifted to lower temperatures as the AC frequency was lowered, indicating slow relaxation of the magnetization of **1** and **2**, characteristic of SCMs. The data from 1.8 to 2.8 K in a zero dc field were fitted by using a generalized Debye model<sup>13</sup> (Figure 4a,b), affording the parameter  $\alpha$  in the range of 0.04–0.14 for **1** and 0.12–0.28 for **2** (see SI). Thus, their relaxation times  $\tau(T)$  have relatively narrow distributions. Similar complexes with an identical bridging motif composed of  $\text{Mn}^{\text{III}}$  salen complexes and carboxylate groups, such as cinnamate, phenylacetate, and benzoate, exhibit no SCM behavior because of the presence of AF long-range ordering.<sup>8</sup> H-bonding between nucleobase

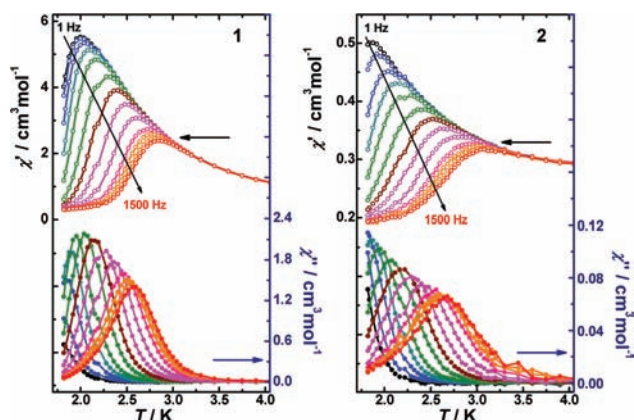


**Figure 3.** Temperature-dependent ac magnetic susceptibility of **1** (left) and **2** (right) with an oscillation of 3 Oe in zero dc magnetic field.

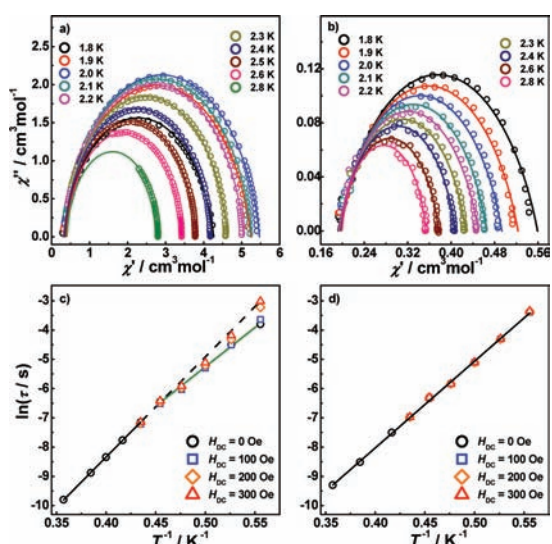


**Figure 4.** Cole–Cole plots of (a) **1** and (b) **2**. The open circles and the solid lines correspond to the experimental data and curves simulated using best fitting parameters, respectively (see SI). Arrhenius plots for (c) **1** and (d) **2**.

moieties of neighboring chains is crucial for SCM behavior in **1** and **2**.

Although the chains of **1** are well-organized with a relatively long interchain distance ( $>12$  Å), an anomaly in the  $\chi''$  vs  $T$  behavior of **1** at low temperatures (Figure 3) was observed. The temperature-dependent behaviors of  $\tau(T)$  of **1** and **2** in the absence of a magnetic field were a little different, although both of them followed the Arrhenius law:  $\tau(T) = \tau_0 \exp(\Delta/kT)$ , where  $\tau_0$  is a prefactor and  $\Delta$  is the activation barrier. For **1**, fitting the data above and below 2.2 K afforded  $\Delta = 34$  and 27 K, respectively (solid black and green lines in Figure 4c), likely caused by the finite-size effect of SCMs.<sup>1</sup> However, by applying a small dc field (ca. 300 Oe),  $\tau(T)$  increased (Figure 5a) and was located on an extension of the fitted line above 2.2 K at zero field (dashed black line in Figure 4c), suggesting an AF ordered phase in **1**. The AF ordered phase was further confirmed on the basis of the derivatives of field-dependent magnetization (Figure S5), field cooling curves (Figure S6), and  $\ln(\chi T)$  vs  $T^{-1}$  plots (Figure 5b) in applied dc magnetic fields of 0–400 Oe. In this range, the maxima of  $\ln(\chi T)$  shifted to lower temperatures and nearly vanished in an applied field of

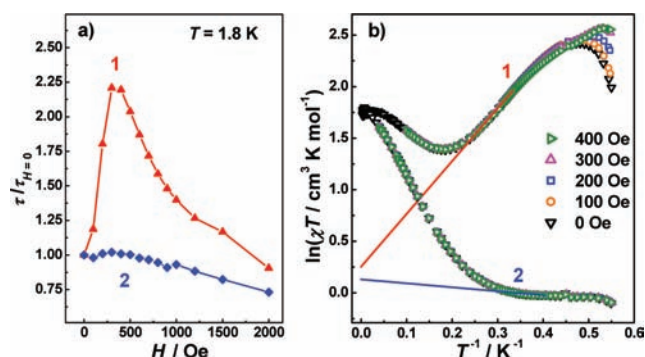


**Figure 5.** (a) Field-dependent relaxation times (normalized at zero field) of **1** and **2** at 1.8 K. (b)  $\ln(\chi T)$  vs  $T^{-1}$  plots for **1** and **2** in applied dc magnetic fields of 0–400 Oe. The solid lines were fitted to the linear portion of the data in a zero field for **1** (red) and **2** (blue).

400 Oe, proving the coexistence of slow relaxation of the magnetization and an AF phase in **1** below 2.2 K.<sup>3</sup> On the other hand, in the case of **2**, no AF ordered state was observed above 1.8 K, and the values of  $\tau(T)$  in the temperature range of 1.8–2.8 K followed the Arrhenius law with  $\Delta = 30$  K (Figure 4d), meaning that **2** is a normal SCM. As mentioned before, the chain packing in **1** and **2** is quite similar, and the interchain distance in **1** is longer than that in **2**, which implies that the interchain H bonds are not the main reason for the higher ordering temperature for **1** than for **2** (vide infra).

As shown in Figure 2c, the 1D chains of **1** and **2** at low temperature can be simplified as non-regular chains with alternating  $J_1$  and  $J_2$ . It has been proposed that  $\Delta = 4(|J_1| \cos(\delta) + J_2)^2 + |D|^2$  for single spin-flip processes when the amplitudes of  $J_1$  and  $J_2$  are similar.<sup>14</sup> By using the obtained values of  $J_1$ ,  $D$ , and  $\delta$  and  $J_2 = 0.2$  K, we calculated  $\Delta = 30$  K for **1** and 32 K for **2**, consistent with the experimental values of 34 and 30 K for **1** and **2**, respectively.

In the 1D uniform F uniaxial anisotropic chain, the correlation length  $\xi$  at low temperatures increased exponentially with decreasing  $T$ , leading to an exponential increase in  $\chi T$  values:  $\chi T \propto \exp(\Delta_\xi/T)$ . Thus, the slope  $\Delta_\xi$  obtained from linear analysis of  $\ln(\chi T)$  vs  $T^{-1}$  is directly related to the exchange contribution for an SCM.<sup>1</sup> However, it has been shown that this linear analysis is not directly related to the exchange contribution for a canted AF SCM.<sup>15</sup> Indeed, the value of  $\Delta_\xi$  obtained by fitting the  $\ln(\chi T)$  vs  $T^{-1}$  plot for **1** in a zero field in the linear region was 5.0 K, whereas the exchange contribution for **1** estimated from  $(\Delta - |D|^2)/2$  was 10.6 K.<sup>16</sup> In addition, the values of  $\chi T$  for **2** did not increase with a decrease in  $T$ , leading to a negative slope ( $-0.38$  K) in the linear region of the  $\ln(\chi T)$  vs  $T^{-1}$  plot (Figure 5b); this behavior is similar to that observed for SCMs of AF chains.<sup>17</sup>

As shown in Figure 2c, the spin vector  $S$  can be decomposed into two components: an uncompensated part ( $S \sin(\delta/2)$ ) and a compensated part ( $S \cos(\delta/2)$ ), which are perpendicular and parallel to the chain, respectively, for  $\delta < 90^\circ$ . As  $T$  was lowered, the 1D F-interacted uncompensated component caused an increase in  $\chi T$ , whereas the compensated component caused  $\chi T$  to decrease monotonically to zero. The experimentally observed  $\chi T$  behavior for a powder sample is due to this competition, and it decreases monotonically with a decrease in  $T$  if  $\delta$  is too small to produce a large enough uncompensated component, which is the case for **2**. On the other hand,  $\ln(\xi)$  along the chain is proportional to  $|J_1| \cos(\delta) +$

$J_2$  in the present case.<sup>1b,14,15</sup> For given  $J_1$  and  $J_2$ , smaller  $\delta$  leads to a steeper increase in  $\xi$  with a decrease in  $T$ . This analysis roughly shows that the relation between  $\chi T$  and  $\xi$  is not straightforward in the present case, and the analysis on  $\chi T$  will seriously underestimate the exchange contribution in the case of small  $\delta$ .

On the other hand, in theory, the deviation of  $\chi T$  and  $\xi$  is advantageous for the preparation of canted AF SCMs. That is, the smaller  $\delta$  hinders 3D ordering in favor of SCM dynamics. It is well known that chains are actually packed in a 3D crystal, and an interchain interaction  $J''$  cannot be eliminated completely because dipolar interactions must be considered.<sup>1c</sup> For a given  $J''$ , the 3D-ordering phase transition temperature  $T_{3D}$  is higher the steeper the divergence of  $\chi_{1D}$  with  $T$ .<sup>18</sup> In the case of a canted AF chain with a small  $\delta$ , the divergence of  $\chi_{1D}$  with  $T$  falls behind that of  $\xi/T$ , and the smaller  $\delta$  is, the more serious lag is. Indeed, the quite similar SCM behaviors of **1** and **2** indicate that they have almost the same divergence of  $\xi/T$  with  $T$ . However, the larger  $\delta$  in **1** makes the divergence of  $\chi_{1D}$  much steeper than that of **2**, leading to a higher phase transition temperature for **1**, even though the interchain distance is greater in **1** than in **2**. This explains why an AF ordered state of SCM was observed for **1** but not for **2** at  $T < 2.2$  K.

In conclusion, two Mn<sup>III</sup> chain complexes with alternating canted AF and F interactions were obtained by linking salen-type Mn<sup>III</sup> out-of-plane dimers with a bridging carboxylate ligand including an adenine moiety. The good organization of chains via H-bonds of adenine moieties between adjacent chains allowed them to behave as SCMs. More importantly, for the first time, we showed that a smaller canting angle hindered 3D ordering in favor of SCM dynamics. Thus, by controlling the structure via H-bonds between nucleobase groups and the intrachain spin arrangement via canting modes, we designed a new SCM system, although similar systems are 3D magnets.<sup>8</sup> The relationship between the size of the canting angle and the observation of SCM behavior is under investigation.

## ■ ASSOCIATED CONTENT

### ● Supporting Information

Crystallographic files in CIF format and additional structural and magnetical data for **1** and **2**. This material is available free of charge via the Internet at <http://pubs.acs.org>.

## ■ AUTHOR INFORMATION

### Corresponding Author

sysuzwx@gmail.com; yamasita@agnus.chem.tohoku.ac.jp

### Notes

The authors declare no competing financial interest.

## ■ ACKNOWLEDGMENTS

We thank Prof. Brian Breedlove (Tohoku University, Sendai, Japan) for helpful discussions. This work was financially supported by a Grant-Aid for Science (S) (Grant No. 20225003) from the Ministry of Education, Culture, Sports, Science, and Technology, Japan. W.-X.Z. is grateful to JSPS for a postdoctoral fellowship.

## ■ REFERENCES

(1) (a) Gatteschi, D.; Sessoli, R.; Villain, J. *Molecular Nanomagnets*; Oxford University Press: New York, 2006. (b) Coulon, C.; Miyasaka, H.; Clérac, R. *Struct. Bonding (Berlin)* **2006**, *122*, 163. (c) Bogani, L.; Vindigni, A.; Sessoli, R.; Gatteschi, D. *J. Mater. Chem.* **2008**, *18*, 4750.

(2) (a) Oshio, H.; Nakano, M. *Chem. Eur. J.* **2005**, *11*, 5178. (b) Milios, C. J.; Vinslava, A.; Wernsdorfer, W.; Prescimone, A.; Wood, P. A.; Parsons, S.; Perlepes, S. P.; Christou, G.; Brechin, E. K. *J. Am. Chem. Soc.* **2007**, *129*, 6547. (c) Klöwer, F.; Lan, Y.; Nehrkorn, J.; Waldman, O.; Anson, C. E.; Powell, A. K. *Chem. Eur. J.* **2009**, *15*, 7413. (d) Kajiwara, T.; Nakano, M.; Takaishi, S.; Yamashita, M. *Inorg. Chem.* **2008**, *47*, 8604.

(3) (a) Coulon, C.; Clérac, R.; Wernsdorfer, W.; Colin, T.; Miyasaka, H. *Phys. Rev. Lett.* **2009**, *102*, 167204. (b) Miyasaka, H.; Takayama, K.; Saitoh, A.; Furukawa, S.; Yamashita, M.; Clérac, R. *Chem. Eur. J.* **2010**, *16*, 3656.

(4) (a) Miyasaka, H.; Saitoh, A.; Yamashita, M.; Clérac, R. *Dalton Trans.* **2008**, 2422. (b) Miyasaka, H.; Madanbashi, T.; Sugimoto, K.; Nakazawa, Y.; Wernsdorfer, W.; Sugiura, K.; Yamashita, M.; Coulon, C.; Clérac, R. *Chem. Eur. J.* **2006**, *12*, 7028. (c) Miyasaka, H.; Julve, M.; Yamashita, M.; Clérac, R. *Inorg. Chem.* **2009**, *48*, 3420.

(5) Lira, E. P.; Huffman, C. W. *J. Org. Chem.* **1966**, *31*, 2188.

(6) Miyasaka, H.; Clérac, R.; Ishii, T.; Chang, H.-C.; Kitagawa, S.; Yamashita, M. *J. Chem. Soc., Dalton Trans.* **2002**, 1528.

(7) (a) Miyasaka, H.; Clérac, R.; Wernsdorfer, W.; Lecren, L.; Bonhomme, C.; Sugiura, K.; Yamashita, M. *Angew. Chem., Int. Ed.* **2004**, *43*, 2801. (b) Lü, Z.-L.; Yuan, M.; Pan, F.; Gao, S.; Zhang, D.-Q.; Zhu, D.-B. *Inorg. Chem.* **2006**, *45*, 3538.

(8) Kar, P.; Guha, P. M.; Drew, M. G. B.; Ishida, T.; Ghosh, A. *Eur. J. Inorg. Chem.* **2011**, 2075.

(9) There are two kinds of out-of-plane dimer moieties, Mn<sup>1</sup>...Mn<sup>1A</sup> and Mn<sup>2</sup>...Mn<sup>2B</sup>, with different metal-metal distances. However, it is very difficult to distinguish them in the analysis of magnetic data. For simplicity, they are assigned as  $J_2$ , since they have similar amplitude when compared with the stronger AF interaction  $J_1$ .

(10) Kennedy, B. J.; Murray, K. *Inorg. Chem.* **1985**, *24*, 1552.

(11) Dzyaloshinsky, I. *J. Phys. Chem. Solids* **1958**, *4*, 241.

(12) The estimated  $\delta$  value is 15° for **1** and 3° for **2**, from the intercept value  $M_u$  obtained by fitting the linear region of the  $M-H$  curve in Figure 2b:  $M_u = M_{\text{sat}} \sin(\delta/2)$ , where  $M_{\text{sat}}$  is saturated magnetization ( $8N\beta$ ). However, the  $M-H$  curves obtained for powder samples will lead to an underestimation of  $\delta$ . Thus, the  $\delta$  values described in text were estimated from the parameters  $J_1$ ,  $D$ , and  $\theta$  by using the equation  $[D \cos(\theta) + 2J_1]/D \sin(\theta) = \cos(\delta)/\sin(\delta)$ : Mossin, S.; Weihe, H.; Sørensen, H. O.; Lima, N.; Sessoli, R. *Dalton Trans.* **2004**, 632.

(13) Cole, K. S.; Cole, R. H. *J. Chem. Phys.* **1941**, *9*, 341.

(14) The Hamiltonian for non-regular alternating Ising chain is  $H = -2J_1 S^2 \sum \sigma_i \sigma_i - 2J_2 S^2 \sum \sigma_i \sigma_{i+1}$ , where  $\sigma_i$  and  $\sigma_{i+1}$  are equal to  $\pm 1$ , so the activation barrier for infinite chain was proposed to be  $\Delta = 4(J_1 + J_2)S^2 + |D|S^2$  when  $J_1$  is comparable with  $J_2$ . As  $J_1$  in the present case is a canted AF interaction,  $|J_1| \cos(\delta)$  is used instead. For detail, see refs 1b and 15.

(15) Bernot, K.; Luzon, J.; Sessoli, R.; Vindigni, A.; Thion, J.; Richeter, S.; Leclercq, D.; Larionova, J.; van der Lee, A. *J. Am. Chem. Soc.* **2008**, *130*, 1619.

(16) In Ising-like canted AF SCM, the equation  $\Delta = 2\Delta_\xi + \Delta_A$  is still valid for single spin-flips in the infinite chain limit, where  $\Delta_A$  is the single ion anisotropy and equals  $|D|S^2$  in the present case.

(17) Some 1D chains of AF-coupled SMMs show the SCM behavior due to intrinsic defects in the materials: (a) Lecren, L.; Roubeau, O.; Coulon, C.; Li, Y.-G.; Le Goff, X. F.; Wernsdorfer, W.; Miyasaka, H.; Clérac, R. *J. Am. Chem. Soc.* **2005**, *127*, 17353. (b) Lecren, L.; Roubeau, O.; Li, Y.-G.; Le Goff, X. F.; Miyasaka, H.; Richard, F.; Wernsdorfer, W.; Coulon, C.; Clérac, R. *Dalton Trans.* **2008**, 755.

(18) The susceptibility of the whole crystal  $\chi_{3D}$  is given by  $\chi_{3D}(T) = \chi_{1D}(T)/[1 - nJ''\chi_{1D}(T)]$  above the magnetic phase transition temperature  $T_{3D}$  where  $\chi_{1D}(T)$  is the susceptibility of an isolated chain and  $n$  is the number of the chains to which the  $J''$  interaction extends. Scalapino, D. J.; Imry, Y.; Pincus, P. *Phys. Rev. B* **1975**, *11*, 2042.